



Optimization and evaluation of reactive dye adsorption on magnetic composite of activated carbon and iron oxide

Roshanak Rezaei Kalanry^{a,b}, Ahmad Jonidi Jafari^b, Ali Esrafil^b, Babak Kakavandi^{c,*}, Abdolmajid Gholizadeh^d, Ali Azari^e

^aCenter for Water Quality Research (CWOR), Institute for Environmental Research (IER), Tehran, University of Medical Sciences, Tehran, Iran, Tel. +98 2186704775; email: rezaei.r@iums.ac.ir (R. Rezaei Kalanry)

^bDepartment of Environmental Health Engineering, School of Public Health, Iran University of Medical Sciences, Tehran, Iran, Tel. +98 2186704775; emails: ahmad_jonidi@yahoo.com (A.J. Jafari), a_esrafil@yahoo.com (A. Esrafil)

^cDepartment of Environmental Health Engineering, School of Health, Ahvaz, Jundishapur University of Medical Sciences, Ahvaz, Iran, Tel. +98 611 3738269; email: kakavandi.b@ajums.ac.ir

^dFaculty of Health, North Khorasan University of Medical sciences, Bojnurd, Iran, Tel. +98 615334566; email: gholizadeh_eng@yahoo.com

^eDepartment of Environmental Health Engineering, School of Public Health, Tehran University of Medical Sciences, Tehran, Iran, Tel. +98 2186704756; email: ali_azari67@yahoo.com

Received 16 April 2014; Accepted 8 January 2015

ABSTRACT

In this study, the magnetic-activated carbon (MAC) was synthesized and employed as an adsorbent for removing Reactive Blue 5 from aquatic environments. Physical properties and surface morphology of the MAC were analyzed using the transmission electron microscopy, scanning electron microscopy (SEM), SEM–energy dispersive analysis by X-ray, X-ray diffraction, vibrating sample magnetometer and Brunauer–Emmett–Teller techniques. The adsorption efficiency of dye was studied in a batch experiment by investigating the influential parameters such as pH, contact time, adsorbent dosage, initial dye concentration, and temperature. Various models of isotherm and kinetic were used to evaluate the obtained data. The equilibrium time was found to be 15 min. The thermodynamic values indicated that the adsorption process was spontaneous and endothermic. The adsorption isotherms and kinetics follow the Langmuir ($R^2 > 0.999$) and pseudo-second-order models ($R^2 > 0.995$), respectively. On conclusion, MAC due to its quick and easy isolation, not leading to the secondary pollution and high efficiency, is a very suitable adsorbent for dye removal from aquatic media.

Keywords: Magnetic composite; Fe₃O₄ nanoparticles; Activated carbon; Adsorption; Reactive Blue 5

1. Introduction

The estimated annual production of dyes across the world is over 700 thousand tons with 10,000 kinds of

color, where 10–15% of these dyes are discharged into the environment along with wastewater produced [1,2]. The presence of dyes in water sources can reduce the penetration of light into water and subsequent reduction of photosynthesis and oxygen, especially in the lower layers, and this would endanger the aquatic

*Corresponding author.

organisms and micro-organisms life [3]. Reactive dyes are one of the most widely used dyes in the textile industries due to the high solubility in water, and thus spreading of these rapidly into the environment has serious economic and environmental effects [4].

Therefore, employing effective and efficient techniques to remove dyes from contaminated aquatic environment is necessary. Methods used for this propose are mainly put in three different categories: physical, chemical, and biological [5]. The chemical methods such as coagulation and flocculation are not suitable for removal of dyes with high solubility in water (e.g. reactive dyes) and often produce high volumes of sludge. The biological methods, because of time-consuming fermentation processes and also their inabilities to remove dyes consistently are not regarded effective and appropriate approaches [6]. The physical methods such as ion exchange, membrane filtration, electrochemical degradation, irradiation, and ozonation are all applied for dye removal. However, these methods are often costly leading to sludge production and hazardous byproducts [7,8].

The adsorption process, is one of the physico-chemical treatment methods, in terms of initial cost, wastewater reuse, simplicity and flexibility in design, easy operation, and not being sensitive to pollutants and toxic compounds, is preferred. The production of high-quality effluent and the absence of hazardous substances such as ozone and free radicals are the major benefits of this approach [9,10]. Yazdanbakhsh et al. reported high efficiency in the adsorption of Reactive Blue 5 (RB5) on perovskite nanoparticles at pH 2 [11]. Tabak et al. also reported an increase in the adsorption of Reactive Blue 15 on a Turkish sepiolite with the rise in temperature and the fall in pH [12]. Powdered-activated carbon (PAC), as an efficient adsorbent, has been suggested for the effective removal of organic contaminants from the aquatic environment, due to its special structure and high adsorption capacity [13]. Unfortunately, the major limitations of using activated carbon and micro- or nano-sized adsorbents are as follows: difficult separation and filtration from the solutions due to small particle size, and secondary turbidity or pollution.

The magnetic property was introduced to the activated carbon through its combination with iron oxide nanoparticles, such as Fe_3O_4 . Recently, magnetic adsorbents and the magnetic separation methods have been widely used because of low cost, simplicity and high speed, and high-efficiency separation [14,15]. So, the researchers have employed this method to remove dyes from the aquatic environment [16,17]. Qu et al. reported that multi-walled carbon nanotubes coated

with Fe_2O_3 nanoparticles had a high efficiency for adsorption of methylene blue and neutral red [8].

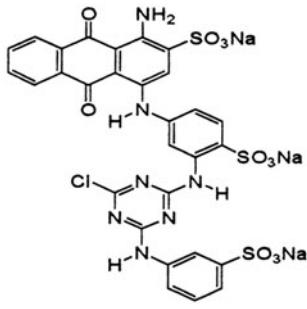
Since the removal of Reactive Blue 5 (RB5) dye using magnetized activated carbon by Fe_3O_4 as adsorbent has not been reported in the literature. So in this work, our aim was to synthesize the magnetic-activated carbon (MAC) as an adsorbent for RB5 removal. The *in vitro* capabilities have been optimized and the studies regarding isotherms, kinetics, and thermodynamic processes were done in detail.

2. Material and methods

2.1. Media and adsorbate preparation

Commercial color index reactive dye RB5 was provided by Arzoo Textile Mills, Faisalabad, Pakistan and used to prepare the stock solution without further purification. Some of the important physico-chemical properties of the investigated dyes are given in Table 1. Iron nitrate ($\text{Fe}(\text{NO}_3)_3 \cdot 9\text{H}_2\text{O}$, 99.9% purity), PAC, and nitric acid (65% HNO_3) were of analytical-laboratory grade, purchased from Merck, Darmstadt, Germany, and was used without further purification for the synthesis of magnetic adsorbent. The pH of solution was adjusted either by adding hydrochloric acid 0.1 M (HCl) or sodium hydroxide 0.1 M (NaOH). A UV-Visible spectrophotometer model CECIL-7100 was applied to determine the dye concentration in the supernatant. The adsorbent was removed from the solution by a magnet (dimension, 5 cm × 4 cm × 4 cm; intensity, 1.3 T).

Table 1
Basic features of the studied dye

Characteristic	
Chemical formula	$\text{C}_{29}\text{H}_{20}\text{ClN}_7\text{O}_{11}\text{S}_3$
Commercial name	Reactive blue 5
Abbreviation	RB5
Class	Anthraquinone
CI number	61,210
Molecular weight (g/mol)	774.16
λ_{max} (nm)	599
Molecular structure	

2.2. Fabrication of MAC and its features

MAC was synthesized according to method given by Do et al. [18] with small alterations. First, a certain amount of PAC was saturated in nitric acid 65% and then homogenized for 3 h at 80°C in the ultrasonic bath. Subsequently, the samples were filtered using a vacuum pump and the powder was saturated in an iron nitrate solution (0.4 g/L) followed by filtration through a paper filter. The filtered samples were then placed in an electric furnace at 750°C for 3 h in the presence of nitrogen gas. The resulting solid product, called synthesized adsorbent, was washed several times with distilled water, dried at 105°C, and finally removed from the solution by a magnet.

X-ray diffraction (XRD) (Quantachrome 2000 NOVA,) was employed to determine the diffraction pattern and the purity of nanoparticles. Magnetic properties of MAC were investigated by a vibrating sample magnetometer (VSM) (7400, Lakeshore, USA) at room temperature. The Brunauer–Emmett–Teller (BET) analysis (Quantachrome, 2000, NOVA) was applied to determine the surface area of the synthesized adsorbent. Adsorbent surface morphology, shape, and size of Fe₃O₄ magnetic nanoparticles coated on the activated carbon were examined by scanning electron microscopy (SEM) (PHILIPS, XL-30) and transmission electron microscopy (TEM) (PHILIPS, EM, 208), respectively. Technique of SEM–EDX (energy dispersive analysis by X-ray, PHILIPS, XL-30) also was used for the characterization of the adsorbent elemental composition.

2.3. Batch adsorption studies

For optimization of several variables such as pH, contact time, temperature, and the adsorbent dosage, the adsorption of RB5 on the MAC was investigated under batch-mode conditions. First, the effect of pH of the solution, ranging from 1 to 11, on the adsorption of 100 mg/L RB5 was evaluated in the presence of 1 g/L MAC. Then, the samples were placed on a shaker (Heidolph, ProMax 2020 model) to get homogenized. The adsorbent was removed from the solution in less than one minute by applying an external magnet. Residual dye concentration in the solution was finally analyzed using UV–visible spectrophotometer (CECIL model 7100) at 592 nm. Afterward, the optimum contact time was obtained at a pre-evaluated pH and subsequently, kinetic modeling was developed by sampling at different time intervals over a period of 180 min. The adsorption isotherms were investigated over various dye concentrations (50–300 mg/L) and MAC dosage of 0.5–2 g/L. Meanwhile, thermody-

amic studies were developed under the optimized conditions. All the samples were measured in duplicate and the mean values were used for the analyses. The percentage of dye removal and the adsorption capacity, q (mg/g), were determined as:

$$q_e = \frac{(C_0 - C_e)V}{W} \quad (1)$$

$$\text{Dye removal (\%)} = \frac{(C_0 - C_e) \times 100}{C_0} \quad (2)$$

where C_0 and C_e are the initial and equilibrium dye concentrations (mg/L), respectively. V is the volume of the solution (L), W is the dry weight of the adsorbent (g), and q_e is the amount of adsorption capacity at equilibrium time (mg/g).

2.4. Adsorption kinetic models

The adsorption kinetics is one the most important issue for understanding both the mechanism of adsorption and the assessment of influential factors on the reaction rate. Three kinetic models, including pseudo-first-order, pseudo-second-order, and Weber–Morris intraparticle diffusion, were used to assess the experimental data. The non-linear forms of the pseudo-first-order and pseudo-second-order equations are given in the following equations:

$$q_t = q_e [1 - \exp(-k_1 t)] \quad (3)$$

$$q_t = q_e - \frac{q_e}{[k_2(q_e)t + 1]} \quad (4)$$

where q_t (mg/g) is the amount of adsorption capacity at a given time t and k_1 , k_2 are the rate constants of pseudo-first-order and pseudo-second-order sorption, respectively. The intraparticle diffusion model can be expressed by the following equation:

$$q_t = k_i \sqrt{t} + C_i \quad (5)$$

where k_i (mg/g min^{0.5}) represents intraparticle diffusion constant. The k_i values were calculated from the slope of the linear region of the curve of q_t vs. $t^{0.5}$, which is directly relative to the rate of adsorption process controlled by intraparticle diffusion. C_i (mg/g) is a constant value depicting the boundary layer effects. If the curve (q_t vs. $t^{0.5}$) is multilinear it implies two or more controlling steps affect the adsorption process [19]. Furthermore, if C_i is equal to zero ($C_i=0$),

intraparticle diffusion is the only rate-determining step. In contrast, $C_i \neq 0$ values suggest that the adsorption process is rather complex and involve more than one diffusive resistance [20].

In this study, apart from correlation coefficient (R^2), the average relative error (ARE) and normalized standard deviation (NSD) were also used as criteria for good fitness. ARE and NSD can be calculated by the following equations, respectively [21]:

$$\text{ARE} = \frac{100}{N} \sum_{i=1}^N \left| \frac{q_{e,\text{exp}} - q_{e,\text{cal}}}{q_{e,\text{exp}}} \right|_i \quad (6)$$

$$\text{NSD} = 100 \sqrt{\frac{1}{N-1} \sum_{i=1}^N \left[\frac{q_{t,\text{exp}} - q_{t,\text{cal}}}{q_{t,\text{exp}}} \right]^2} \quad (7)$$

where $q_{e,\text{exp}}$ and $q_{e,\text{cal}}$ are the batch experimental and calculated amounts of RB5 adsorbed on MAC at equilibrium condition, respectively. $q_{t,\text{exp}}$ and $q_{t,\text{cal}}$ are the corresponding values at a given time t . N represents the number of the measurements [22].

2.5. Adsorption isotherm models

The adsorption isotherms are characterized by certain constant values. These values express the surface properties and the affinity of the adsorbent. Herein, Langmuir, Freundlich, and Temkin models were employed to analyze the equilibrium data. The Langmuir model is obtained under the ideal assumption (i.e. total homogeneous monolayer surface adsorption), which can be expressed by:

$$q_e = \frac{q_0 K_L C_e}{1 + K_L C_e} \quad (8)$$

where q_0 is the maximum amount of adsorption (mg/g) and K_L is the adsorption equilibrium constant (L/mg). The fundamental properties of the Langmuir isotherm can be explained in terms of dimensionless separation factor R_L ; ($R_L = 1/(1 + K_L C_0)$). The type of isotherm is indicated by R_L values, which is as follows:

Unfavorable ($R_L > 1$), favorable ($0 < R_L < 1$), irreversible ($R_L = 0$), and linear adsorption ($R_L = 1$) [23].

The empirical Freundlich model is based upon the assumption of multilayer formation of adsorbate on the heterogeneous solid surface of the adsorbent and assumes that the stronger binding sites are occupied

first, and then the binding strength decreases with the rise in the degree of site occupation. A non-linear form of the Freundlich isotherm equation is expressed as follows:

$$q_e = K_F C_e^{1/n} \quad (9)$$

where K_F and n are the adsorption capacity and the adsorption intensity, respectively. The lower fractional value of n ($0 < n < 1$) indicates that weak adsorptive forces are effective on the surface of the MAC, the number of adsorption sites on the surface are limited, and the adsorbed dye may hinder the further adsorption. For $n = 2-10$ and $1-2$, adsorption is favorable and moderately difficult, respectively [24].

The Temkin model considers the effects of some indirect adsorbate–adsorbent interactions on the adsorption isotherms. As a result of adsorbate–adsorbent interactions, the heat of adsorption of all the molecules in the layer would decrease linearly with the coverage. The linear form of the Temkin isotherm is represented by the following equation:

$$q_e = B \ln(k_T C_e) \quad (10)$$

k_T is binding constant which represents the maximum binding energy (L/mg) and B ($B = RT/b_T$) is Temkin constant which is dependent on temperature. R is the universal gas constant (8.314 J/mol K) and T is the absolute temperature degree (K).

2.6. Adsorption thermodynamic study

To study the adsorption thermodynamics, three main parameters such as change in Gibb's free energy (ΔG°), enthalpy (ΔH°), and entropy (ΔS°) were calculated using the following equations:

$$\ln k_L = \frac{\Delta S^\circ}{R} - \frac{\Delta H^\circ}{RT} \quad (11)$$

where k_L (q_e/C_e) is the distribution coefficient, q_e is the amount of RB5 adsorbed at equilibrium (mg/g), and C_e is the equilibrium concentration of RB5 in the solution (mg/L). The values of ΔH° and ΔS° can be calculated from the intercept and slope of Vant Hoff plots of $\ln k_L$ vs. $1/T$, respectively. The standard ΔG° can be calculated using the below equation:

$$\Delta G^\circ = -RT \ln k_L \quad (12)$$

3. Results and discussion

3.1. MAC properties

The XRD analysis results obtained using Cu-K α radiation at 25°C, shown in Fig. 1(a), revealed that the maximum peak (at 35.5°) was related to cubic iron oxide crystals, according to the standard (No. 0866-088-01JCPDS). The XRD pattern confirmed the presence of Fe₃O₄ particles with purity of 100% within the structure of PAC. Fig. 1(b) shows the VSM magnetization curve of the prepared adsorbent at 25°C in the cycling magnetic field of -10 to +10 kOe. The highest saturation magnetization obtained for MAC was 6.94 emu/g underlying superparamagnetic characteristic [25]. These results also suggested that the MAC had shown excellent magnetic response to a magnetic field. So, this magnetic composite could be applied as an adsorbent in environmental purposes and then it could be easily and rapidly removed from the solution (Fig. 1(c)).

Fig. 2(a) and (b) shows the SEM image of MAC at 25 keV and the TEM image of Fe₃O₄ at 100 keV, respectively. The SEM image shows uniform

distribution of pores on the activated carbon and suggests good porosity of the synthesized adsorbent. As shown in Fig. 2(b), the morphology of MAC depicts the fine Fe₃O₄ particles of less than 80 nm diameter with a cubic structure. The cubic structure is consistent with the results obtained from XRD analysis. The analysis of SEM-EDX (Fig. 2 (c)) confirms the presence of elements such as carbon, oxygen, iron, lead, and zinc in the MAC structure. Created peaks for iron in this analysis also confirm the presence of Fe element on the PAC surfaces. It also revealed the presence of 71.6 carbon, 8.3 oxygen, and 20.1% iron, in adsorbent structure. Thus, these results suggest that approximately 28% of the surface of PAC has been occupied by iron which was in the form of Fe₃O₄ nanoparticles. The specific surface area of the MAC was measured 671.2 m²/g using BET analysis. Fig. 2(d) indicates the nitrogen adsorption-desorption isotherms of MAC. The figure exhibits type IV isotherm for prepared adsorbent according to classification of the IUPAC indicating that MAC structure is typically mesoporous [17].

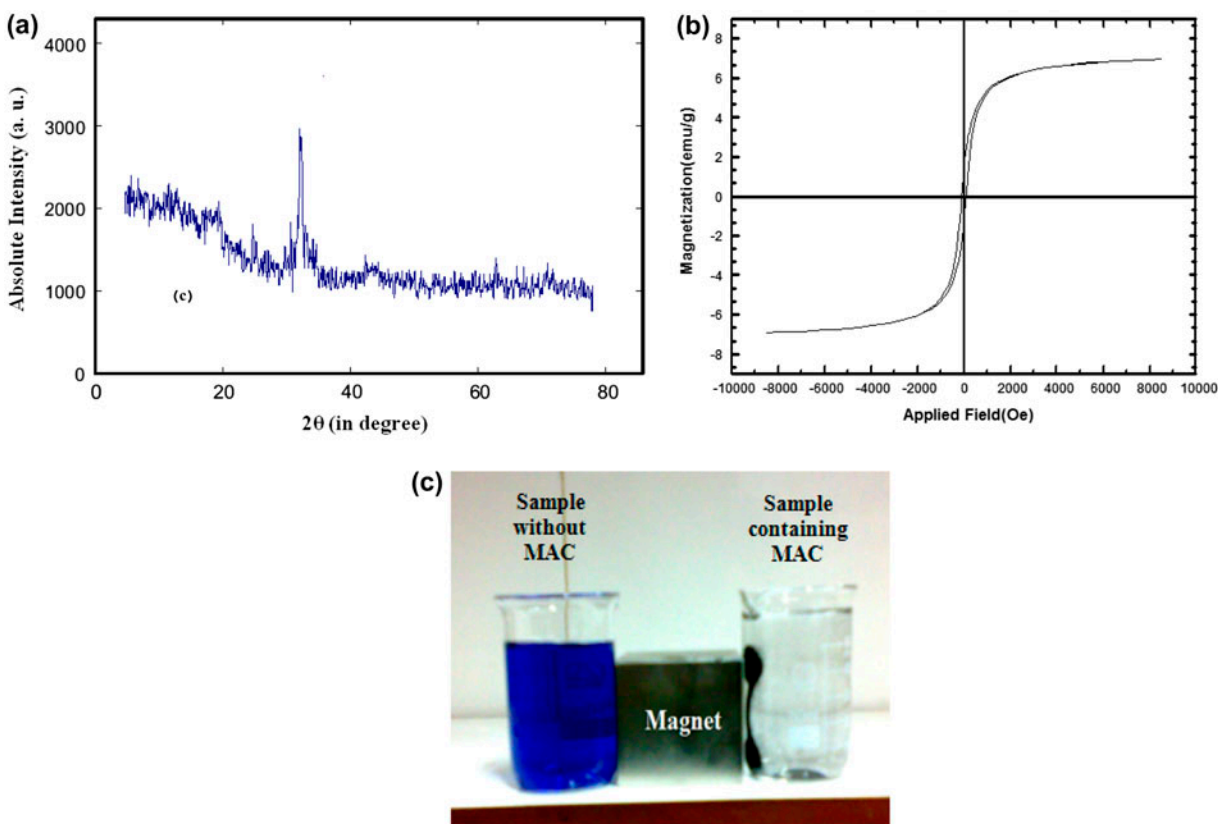


Fig. 1. (a) X-ray diffraction, (b) magnetic hysteresis cycle, and (c) performance of magnet in the magnetic separation of adsorbent from solution.

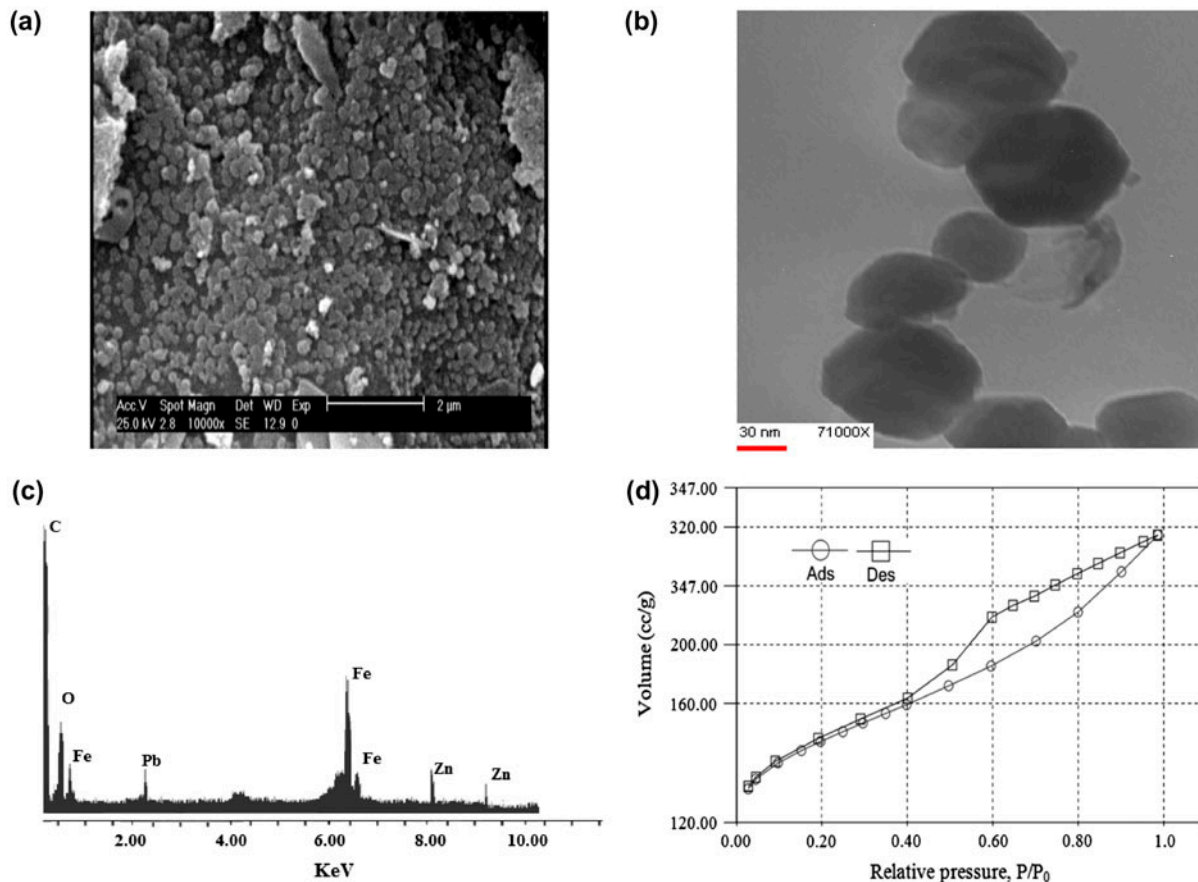


Fig. 2. The analysis of SEM (a), TEM (b), and SEM–EDX (c), for MAC and N₂ adsorption–desorption isotherms of MAC (d).

3.2. Effect of pH

pH of the solution plays an important role in adsorption process. It can affect the solution chemistry and adsorbent surface charge and functional groups on the active sites. The effect of pH variations on the adsorption of RB5 onto the MAC revealed that the adsorption process has better efficiency at acidic conditions. Fig. 3 shows that the rise in the pH from 1 to 11 leads to the fall in the adsorption capacity from 91.3 to 48.4 mg/g, respectively. The high adsorption efficiency at pH of 3 can be attributed to the electrostatic attraction between negatively charged dye molecules and the positively charged MAC surface. At higher pH, however, the electrostatic repulsion between the negatively charged adsorbed ions and the negatively charged adsorbent surface reduces the dye adsorption [26,27]. It is worth noting that the optimum acidic pH has also been reported in previous

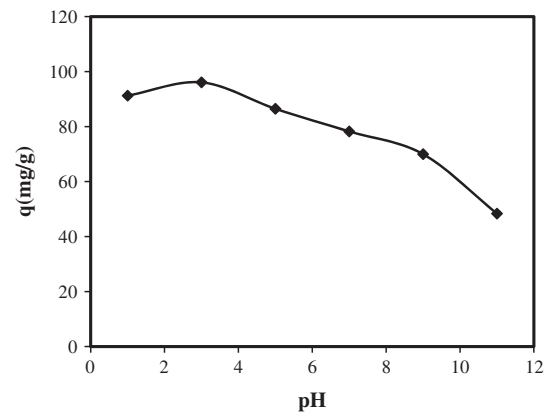


Fig. 3. Effect of the pH on the adsorption of RB5 onto MAC ($C_0 = 100$ mg/L, $t = 60$ min, adsorbent dosage (m) = 1 g/L, and $T = 20^\circ\text{C}$).

studies [11]. Therefore, pH 3 was chosen as optimum for the subsequent adsorption experiments.

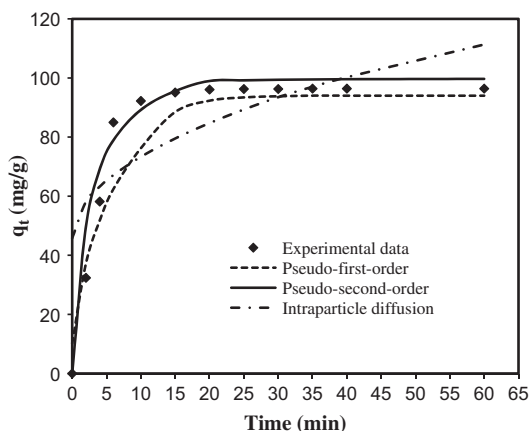


Fig. 4. The plots of kinetic models for RB5 adsorption onto MAC (pH 3, $m = 1$ g/L, $C_0 = 100$ mg/L, and $T = 20^\circ\text{C}$).

3.3. Effect of contact time and adsorption kinetics

The effect of contact time on the adsorption capacity of RB5 onto MAC (Fig. 4) revealed that the sorption process was very fast. This phenomenon may be attributed to a sufficient number of unsaturated active sites on the MAC. As shown in Fig. 4, huge amounts of RB5 were adsorbed onto MAC within the first 10–15 min, so 15 min was chosen as the equilibrium time. The values of kinetic parameters regarding RB5 adsorption onto MAC in Table 2 shows that the adsorption process follows pseudo-second-order model based on the correlation coefficient (R^2). The plots of kinetic adsorption (Fig. 4) also suggest that the experimental data regarding the RB5 adsorption onto the MAC are in agreement with pseudo-second-order model. This result indicates that the adsorption process is controlled by chemisorption [15,28]. The chemisorption is the sharing or exchange of electrons between the dye molecules and the binding sites of MAC, as reported by Konicki et al. [29].

The less ARE and NSD values of the pseudo-second-order, in comparison with the others, confirm that

more accurate values of q_t are obtained in the pseudo-second-order. This model suggests that two steps happen in the adsorption process either in series or parallel. The first step is fast and reaches the equilibrium state quickly, which could be due to the diffusion of the dye molecules from the solution phase to the external surface of MAC, while the second step is relatively slow that could continue for a long period of time [21,30]. Amin studied the removal of Direct Blue color-06 using activated carbon, and they reported pseudo-second-order as being the appropriate kinetic model [31].

3.4. Mechanism of RB5 adsorption

Generally, the process of adsorption of adsorbate onto adsorbent occurs through multistep mechanism involving: (a) outer (external) film diffusion, (b) intraparticle mass transfer, and (c) adsorbate sorption on active site (chemical sorption) [19,32]. Since the external film diffusion is resulted from agitation of the solution, the rate-limiting step seems to be intraparticle diffusion and/or sorption on the active site [32]. It is clear from Table 2 that value of regression coefficient for intraparticle diffusion model was lower than 0.6 indicating that the intraparticle diffusion was not the only rate-determining step [33]. The positive value of C_i ($C_i = 51.6$ mg/g) implies that the not limited effect of mechanisms other (i.e. chemical sorption or external mass transfer) on the adsorption rate [32].

3.5. Effect of MAC and RB5 different concentrations

The effects of adsorbent and adsorbate concentration on the adsorption efficiency were investigated at equilibrium time (15 min and the optimum pH 3) in the range of 0.5–2 g/L and 50–300 mg/L, respectively. Fig. 5 shows that with the increase in MAC dosage from 0.5 to 2 g/L, the adsorption efficiency of RB5 100 mg/L increases from 81.6 to 100%. The enhancement in the adsorption can be due to rise in the

Table 2
Kinetic parameters of RB5 adsorption onto the MAC

Kinetic models														
Pseudo-first-order					Pseudo-second-order					Intraparticle diffusion				
$q_{e,cal}$ (mg/g)	K (min ⁻¹)	R^2	ARE	NSD	$q_{e,cal}$	K2 (g/mg) (min ⁻¹)	R^2	ARE	NSD	k_i	C_i	R^2	ARE	NSD
86.05	0.19	0.953	3.2	6.74	100	0.005	0.996	1.7	3.6	8.7	45.78	0.688	5.48	11.61
$q_{e,exp}$ (mg/g)					95.12									

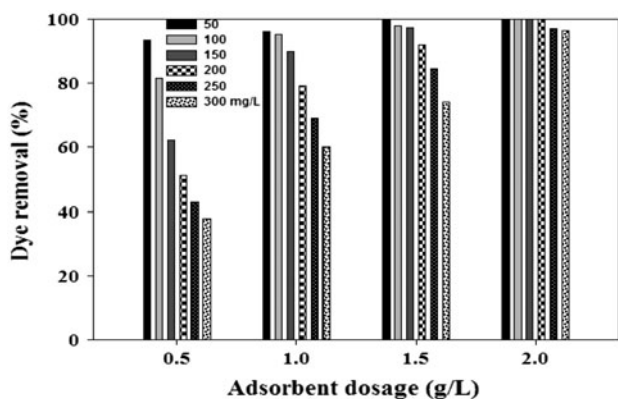


Fig. 5. The effect of RB5 and MAC concentrations on the adsorption efficiency (pH 3, $t = 15$ min, and $T = 20^\circ\text{C}$).

adsorption surface rate, and consequently the RB5's broad access to the adsorption sites on MAC [34,35]. We did not observe significant difference in the removal efficiency of 50 and 100 mg/L concentrations of RB5 dye when the adsorbent dosage increased from 1 to 2 g/L. Therefore, the amount of MAC 1 g/L was selected as optimized dosage of the adsorbent for the adsorption process. Fig. 5 also indicates that the percentage of dye adsorption was decreased from 96 to 60% when initial RB5 concentration was increased from 50 to 300 mg/L (on 1 g/L of MAC). This is probably due to the fixed number of active sites on the adsorbent vs. to increase in the number of dye molecules [35]. In the study of Direct Yellow 12 adsorption onto silver nanoparticles-loaded activated carbon, Ghaedi et al. [36] showed that the adsorption efficiency increased by increasing the adsorbent dosage and decreasing initial amoxicillin concentration.

3.6. Adsorption isotherms

Equilibrium isotherm equations were used to describe the adsorption of RB5 in the range of 50–300 mg/L onto the MAC at dosage of 1 g/L. The values of isotherm parameters at different temperatures are listed in Table 3. Three models best fitting

the equilibrium data were assessed based on the regression coefficient (R^2). Among the models, the Langmuir showed more validity than the other two at all studied temperatures, and it also showed a fair agreement with experimental data. Fig. 6 also confirms the very good correspondence between experimental data and Langmuir isotherm model at different temperatures of the solution. These findings imply the uniform distribution of homogeneous active sites on the adsorbent surface [37]. The rises in the adsorption capacity regarding the Langmuir model along with the rise in the temperature confirm that the adsorption process is endothermic. Other researchers reported that the Langmuir isotherm was the best model for the adsorption of reactive dyes on activated carbon as well [27,38,39]. The R_L values fall between 0 and 1; so, the adsorption of RB5 molecules onto MAC is desirable [15].

3.7. Comparison with other adsorbents

A comparison between adsorption capacities of the synthesized adsorbent in this work with different adsorbents for the removal of RB5 dye reported in the literature are listed in Table 4. The maximum amount of RB5 uptake per unit mass of the MAC was 250 mg/g based on the Langmuir equilibrium model at 50°C . It is noticeable from Table 4 that the MAC has a good maximum adsorption capacity in comparison with other adsorbents. So, it can be employed as a promising adsorbent to remove organic dyes.

3.8. Impact of solution temperature and adsorption thermodynamics

The effect of temperature on the adsorption of RB5 using MAC is shown in Fig. 7. It was noted that by increasing the temperature from 20 to 50°C , the adsorption capacity enhanced up to 216 mg/g. This observation implies that the RB5 adsorption onto MAC may be a kinetically controlled process [40]. Rise in the temperature leads to an increase in pollutants

Table 3

Obtained data with respect to the equilibrium isotherms for the adsorption RB5 onto the MAC

T ($^\circ\text{C}$)	Langmuir				Freundlich			Temkin		
	q_m (mg/g)	K_L (L/mg)	R^2	R_L	K_F (mg/g (L/mg)) $^{1/n}$	n	R^2	k_T	B	R^2
20	200	0.16	0.999	0.02–0.12	49.95	3.36	0.973	3.36	31.58	0.973
30	200	0.357	0.999	0.01–0.05	64.13	3.58	0.874	7.43	31.65	0.874
40	250	0.285	0.999	0.01–0.06	66.38	3.28	0.948	5.96	36.84	0.948
50	250	0.34	0.999	0.01–0.05	69.96	3.27	0.946	6.68	37.47	0.946

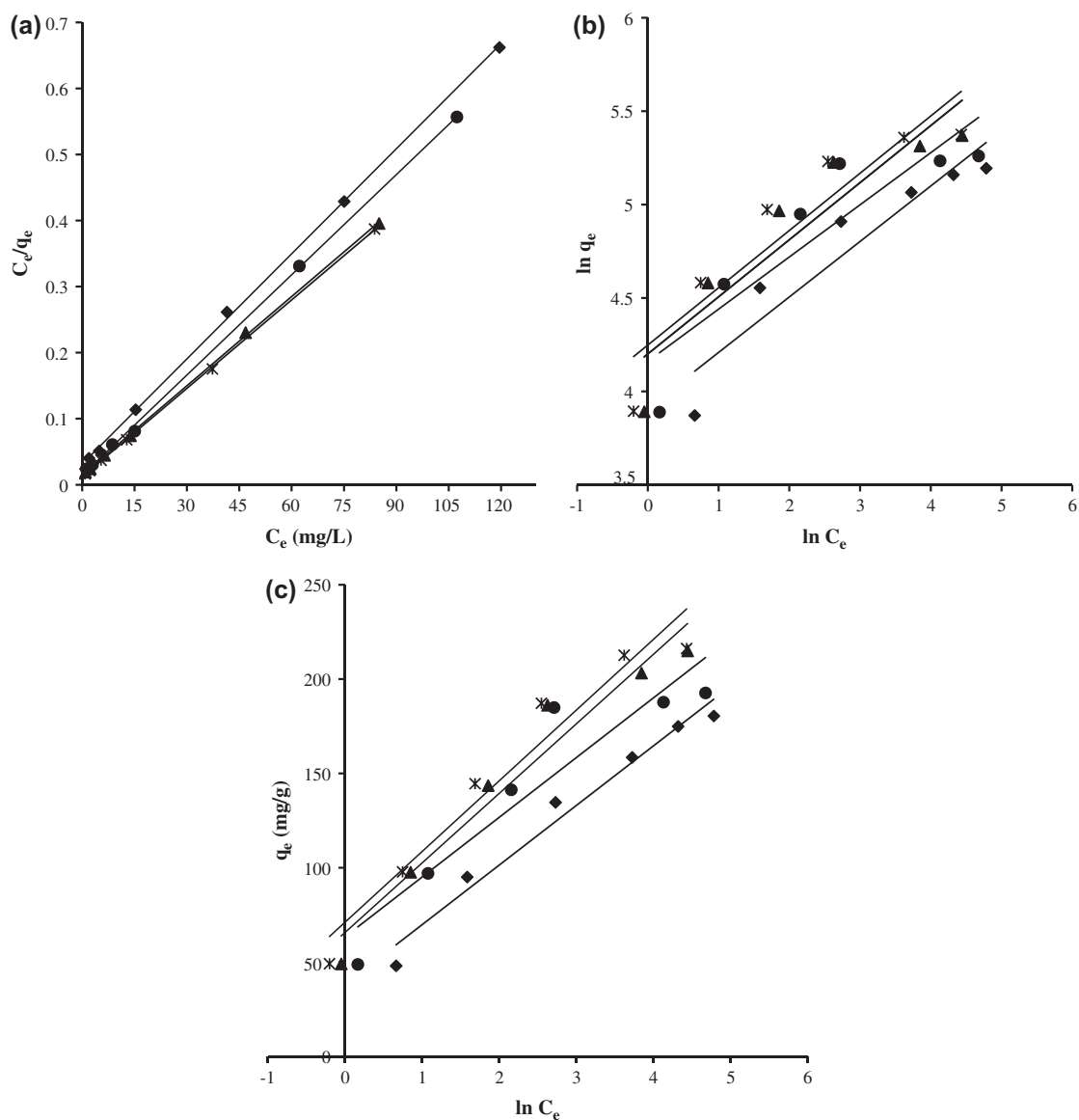


Fig. 6. Isotherm plots of RB5 adsorption onto MAC: (a) Langmuir isotherm, (b) Freundlich isotherm, and (c) Temkin isotherm (MAC dosage = 1 g/L, initial pH 3, contact time = 15 min, initial dye concentration = 50–300 mg/L, and temperature = \blacklozenge 20°C, \bullet 30°C, \blacktriangle 40°C, and $*$ 50°C).

Table 4

Comparison of adsorption capacity of RB5 between various adsorbents found in the literatures

Adsorbent	Isotherm	Kinetic	q_m (mg/g)	References
$\text{La}_{0.5}\text{Ca}_{0.5}\text{NiO}_3$	Langmuir	Pseudo-second-order	36.23	[11]
ZnCr_2O_4 nanoparticles	Langmuir	Pseudo-second-order	41.32	[40]
$\text{LiCo}_{0.5}\text{Fe}_{0.5}\text{O}_2$	Freundlich	Pseudo-second-order	76.92	[40]
MAC	Langmuir	Pseudo-second-order	250	This work

uptake through the following ways: (1) increasing the mobility of the dye followed by an increase in the effective interactions between the reacting and the

adsorbent material and (2) increasing the pore size of the adsorbent surface [41,42]. Similar results were also reported by other researchers in the cases of

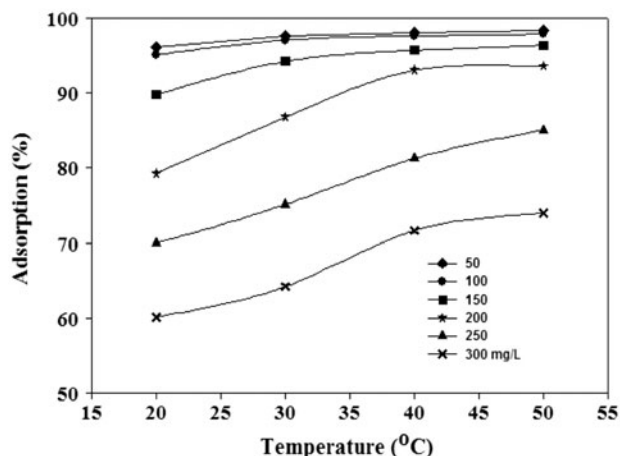


Fig. 7. Effect of temperature solution on the adsorption RB5 using MAC (pH 3, $t = 15$ min, $C_0 = 50$ – 300 mg/L, and $m = 1$ g/L).

methylene blue dye removal using montmorillonite/ CoFe_2O_4 composite, as well as the removal of Reactive Black 5 dye using magnetic chitosan resins [14,32].

The plot of Van't Hoff ($\ln k_p$ vs. $1/T$) to determine the thermodynamic parameters for RB5 adsorption process is shown in Fig. 8. The calculated values of the thermodynamic parameters are presented in Table 5. ΔH° has a positive value implying that the adsorption process was endothermic and also suggesting that there should be a strong chemical bond between the dye molecules and the adsorbent surface [43]. Meanwhile, the positive values of ΔS° indicate the fact of uniform distribution of the adsorbent surface [32,39]. However, the negative values obtained

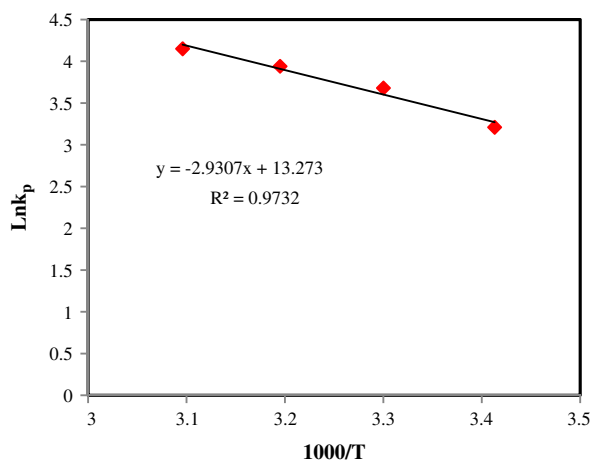


Fig. 8. The Van't Hoff plot for adsorption process of RB5 onto MAC (pH 3, $t = 15$ min, $C_0 = 50$ mg/L, and $m = 1$ g/L).

for the ΔG° demonstrates that the adsorption of RB5 on MAC is spontaneous. The sharp decline in ΔG° values with increasing temperature is may be due to the fact that the dehydration of both adsorbate and adsorbent. This latter phenomenon facilitates the reaction led by favorable adsorption at higher temperatures [10].

3.9. Reusability of MAC

Reusability of adsorbents is important for economic and resource reasons. The adsorbent reusability and desorption of RB5 dye loaded on MAC were performed using six adsorption–desorption cycles. Here, first the performance of RB5 adsorption was investigated with an initial dye concentration of 50 mg/L under optimal conditions (pH 3, contact time of 15 min, and adsorbent dose of 1 g/L) for six consecutive cycles. After the equilibrium adsorption, adsorbent was magnetically separated from solution and the liquid phase was analyzed by a spectrophotometer. At the end of each cycle of the adsorption, desorption experiments were then carried out using 0.1 M HCl as a desorbing solution. In this way, 0.1 g of MAC loaded with RB5 dye added to 10 ml of 0.1 M HCl solution and was placed on a shaker for 12 h, at 200 rpm, and $25 \pm 1^\circ\text{C}$. The reason for choosing the above-mentioned desorption solution was to avoid damage to the adsorbent and/or physical changes of the structure. The desorption percentage (%) was calculated using the ratio of the weight of RB5 desorbed and the weight of RB5 adsorbed, as follows:

$$\text{Desorption (\%)} = \frac{\text{Desorbed RB5 (mg)}}{\text{Adsorbed RB5 (mg)}} \quad (13)$$

As shown Fig. 9, the reusability of adsorbent did not significantly change during the six adsorption–desorption cycles. So, the adsorption percentage of RB5 dye by MAC decreased from 97.2 to 86.7% after six cycles. This suggests that the MAC can be recycled and reused for a maximum of six successive cycles with an adsorption efficiency $>86\%$. It was also observed

Table 5

The values of thermodynamic parameters for RB5 adsorption onto the MAC

ΔG° (kJ/mol)				ΔH° (kJ/mol)	ΔS° (kJ/mol K)
20	30	40	50		
−7.82	−9.27	−10.25	−11.14	24.36	0.11

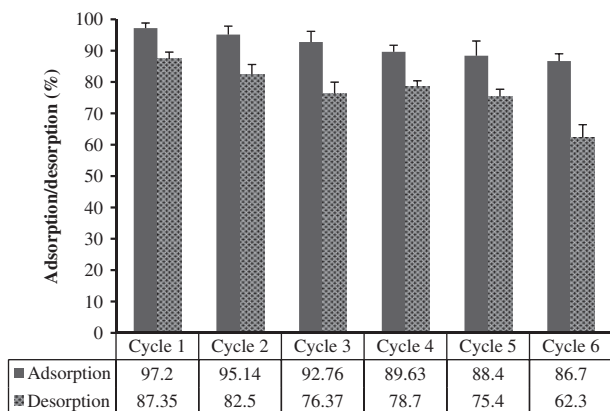


Fig. 9. Percentage of RB5 dye adsorbed–desorbed per cycle (pH 3, $t = 15$ min, $C_0 = 50$ mg/L, and $m = 1$ g/L).

that more than 62.3% of RB5 adsorbed could be desorbed and recovered from the adsorbent surface in the presence of HCl in the sixth cycle. The high desorption percentage may be due to the protonation of surface adsorbent with acidic agent [44]. Therefore, MAC can serve as an economical and effective adsorbent for RB5 removal from aqueous solutions in industrial applications based on simple and easy regeneration.

4. Conclusion

In this study, the combination of activated carbon and iron oxide nanoparticles was used as an adsorbent for the removal of RB5 from aquatic environments. Adsorption studies revealed that the best removal efficiency was obtained at acidic pH. After 15 min, the adsorption reaction reached the equilibrium state. The studies of adsorption isotherm and kinetic models showed that the RB5 adsorption onto MAC obeys Langmuir isotherm and pseudo-second-order kinetic models. Also, the results obtained from the thermodynamic parameters showed that the dye adsorption was enhanced with an increase in temperature, and it was endothermic and spontaneous in nature. Since widespread use of PAC as adsorbent for the removal of pollutants is already well known, it is expected that the magnetization of the activated carbon particles neither alters its physical properties nor its surface. Subsequently, they could be applied for solving the problems associated with the separation and filtration.

References

[1] X. Luo, Y. Zhan, Y. Huang, L. Yang, X. Tu, S. Luo, Removal of water-soluble acid dyes from water

environment using a novel magnetic molecularly imprinted polymer, *J. Hazard. Mater.* 187 (2011) 274–282.

- [2] G. McMullan, C. Meehan, A. Conneely, N. Kirby, T. Robinson, P. Nigam, I. Banat, R. Marchant, W. Smyth, Microbial decolourisation and degradation of textile dyes, *Appl. Microbiol. Biotechnol.* 56 (2001) 81–87.
- [3] K.P. Singh, S. Gupta, A.K. Singh, S. Sinha, Optimizing adsorption of crystal violet dye from water by magnetic nanocomposite using response surface modeling approach, *J. Hazard. Mater.* 186 (2011) 1462–1473.
- [4] J.-L. Gong, B. Wang, G.-M. Zeng, C.-P. Yang, C.-G. Niu, Q.-Y. Niu, W.-J. Zhou, Y. Liang, Removal of cationic dyes from aqueous solution using magnetic multi-wall carbon nanotube nanocomposite as adsorbent, *J. Hazard. Mater.* 164 (2009) 1517–1522.
- [5] M.A. Ahmad, R. Alrozi, Removal of malachite green dye from aqueous solution using rambutan peel-based activated carbon: Equilibrium, kinetic and thermodynamic studies, *Chem. Eng. J.* 171 (2011) 510–516.
- [6] P. Bahmani, R.R. Kalantry, A. Esrafil, M. Gholami, A.J. Jafari, Evaluation of Fenton oxidation process coupled with biological treatment for the removal of reactive black 5 from aqueous solution, *J. Environ. Health Sci. Eng.* 11 (2013) 1–13.
- [7] B. Hameed, M. El-Khaiary, Equilibrium, kinetics and mechanism of malachite green adsorption on activated carbon prepared from bamboo by K(2)CO(3) activation and subsequent gasification with CO(2), *J. Hazard. Mater.* 157 (2008) 344–351.
- [8] S. Qu, F. Huang, S. Yu, G. Chen, J. Kong, Magnetic removal of dyes from aqueous solution using multi-walled carbon nanotubes filled with Fe₂O₃ particles, *J. Hazard. Mater.* 160 (2008) 643–647.
- [9] M. Shirmardi, A. Mesdaghinia, A.H. Mahvi, S. Nasser, R. Nabizadeh, Kinetics and equilibrium studies on adsorption of acid red 18 (Azo-Dye) using multiwall carbon nanotubes (MWCNTs) from aqueous solution, *J. Chem.* 9 (2012) 2371–2383.
- [10] B. Kakavandi, R. Rezaei Kalantry, M. Farzadkia, A.H. Mahvi, A. Esrafil, A. Azari, A.R. Yari, A.B. Javid, Enhanced chromium (VI) removal using activated carbon modified by zero valent iron and silver bimetallic nanoparticles, *J. Environ. Health Sci. Eng.* 12 (2014) 1–10.
- [11] M. Yazdanbakhsh, H. Tavakkoli, S.M. Hosseini, Characterization and evaluation catalytic efficiency of La_{0.5}Ca_{0.5}NiO₃ nanopowders in removal of reactive blue 5 from aqueous solution, *Desalination* 281 (2011) 388–395.
- [12] A. Tabak, E. Eren, B. Afsin, B. Caglar, Determination of adsorptive properties of a Turkish sepiolite for removal of reactive blue 15 anionic dye from aqueous solutions, *J. Hazard. Mater.* 161 (2009) 1087–1094.
- [13] K. Foo, B.H. Hameed, An overview of dye removal via activated carbon adsorption process, *Desalin. Water Treat.* 19 (2010) 255–274.
- [14] L. Ai, Y. Zhou, J. Jiang, Removal of methylene blue from aqueous solution by montmorillonite/CoFe₂O₄ composite with magnetic separation performance, *Desalination* 266 (2011) 72–77.
- [15] B. Kakavandi, A. Esrafil, A. Mohseni-Bandpi, A.J. Jafari, R.R. Kalantry, Magnetic Fe₃O₄@C nanoparticles as adsorbents for removal of amoxicillin from aqueous solution, *Water Sci. Technol.* 69 (2014) 147–155.

- [16] P.R. Chang, P. Zheng, B. Liu, D.P. Anderson, J. Yu, X. Ma, Characterization of magnetic soluble starch-functionalized carbon nanotubes and its application for the adsorption of the dyes, *J. Hazard. Mater.* 186 (2011) 2144–2150.
- [17] V. Rocher, J.-M. Siaugue, V. Cabuil, A. Bee, Removal of organic dyes by magnetic alginate beads, *Water Res.* 42 (2008) 1290–1298.
- [18] M.H. Do, N.H. Phan, T.D. Nguyen, T.T.S. Pham, V.K. Nguyen, T.T.T. Vu, T.K.P. Nguyen, Activated carbon/ Fe_3O_4 nanoparticle composite: Fabrication, methyl orange removal and regeneration by hydrogen peroxide, *Chemosphere* 85 (2011) 1269–1276.
- [19] A.W. Ip, J.P. Barford, G. McKay, A comparative study on the kinetics and mechanisms of removal of reactive black 5 by adsorption onto activated carbons and bone char, *Chem. Eng. J.* 157 (2010) 434–442.
- [20] A. Rodríguez, J. García, G. Ovejero, M. Mestanza, Adsorption of anionic and cationic dyes on activated carbon from aqueous solutions: Equilibrium and kinetics, *J. Hazard. Mater.* 172 (2009) 1311–1320.
- [21] A. Behnamfard, M.M. Salarirad, Equilibrium and kinetic studies on free cyanide adsorption from aqueous solution by activated carbon, *J. Hazard. Mater.* 170 (2009) 127–133.
- [22] K.V. Kumar, K. Porkodi, F. Rocha, Isotherms and thermodynamics by linear and non-linear regression analysis for the sorption of methylene blue onto activated carbon: Comparison of various error functions, *J. Hazard. Mater.* 151 (2008) 794–804.
- [23] B. Kakavandi, A. Jonidi Jafari, R. Rezaei Kalantry, S. Nasser, A. Ameri, A. Esrafi, Synthesis and properties of Fe_3O_4 -activated carbon magnetic nanoparticles for removal of aniline from aqueous solution: Equilibrium, kinetic and thermodynamic studies, *J. Environ. Health Sci. Eng.* 10 (2013) 1–9.
- [24] B. Hameed, D. Mahmoud, A. Ahmad, Equilibrium modeling and kinetic studies on the adsorption of basic dye by a low-cost adsorbent: Coconut (*Cocos nucifera*) bunch waste, *J. Hazard. Mater.* 158 (2008) 65–72.
- [25] T. Depci, Comparison of activated carbon and iron impregnated activated carbon derived from Gölbaşı lignite to remove cyanide from water, *Chem Eng J.* 181 (2012) 467–478.
- [26] Y.S. Al-Degs, M.I. El-Barghouthi, A.H. El-Sheikh, G.M. Walker, Effect of solution pH, ionic strength, and temperature on adsorption behavior of reactive dyes on activated carbon, *Dyes Pigm.* 77 (2008) 16–23.
- [27] H. Xiao, H. Peng, S. Deng, X. Yang, Y. Zhang, Y. Li, Preparation of activated carbon from edible fungi residue by microwave assisted K_2CO_3 activation—Application in reactive black 5 adsorption from aqueous solution, *Bioresour. Technol.* 111 (2012) 127–133.
- [28] X.-J. Hu, Y.-G. Liu, H. Wang, A.-W. Chen, G.-M. Zeng, S.-M. Liu, Y.-M. Guo, X. Hu, T.-T. Li, Y.-Q. Wang, Removal of Cu (II) ions from aqueous solution using sulfonated magnetic graphene oxide composite, *Sep. Purif. Technol.* 108 (2013) 189–195.
- [29] W. Konicki, I. Petech, E. Mijowska, I. Jasińska, Adsorption kinetics of acid dye acid red 88 onto magnetic multi-walled carbon nanotubes- Fe_3C nanocomposite, *CLEAN—Soil Air Water* 42 (2014) 284–294.
- [30] Y. Khambhaty, K. Mody, S. Basha, B. Jha, Kinetics, equilibrium and thermodynamic studies on biosorption of hexavalent chromium by dead fungal biomass of marine *Aspergillus niger*, *Chem. Eng. J.* 145 (2009) 489–495.
- [31] N.K. Amin, Removal of reactive dye from aqueous solutions by adsorption onto activated carbons prepared from sugarcane bagasse pith, *Desalination* 223 (2008) 152–161.
- [32] K.Z. Elwakeel, Removal of Reactive Black 5 from aqueous solutions using magnetic chitosan resins, *J. Hazard. Mater.* 167 (2009) 383–392.
- [33] H.-Y. Zhu, R. Jiang, L. Xiao, W. Li, A novel magnetically separable $\gamma\text{-Fe}_2\text{O}_3$ /crosslinked chitosan adsorbent: Preparation, characterization and adsorption application for removal of hazardous azo dye, *J. Hazard. Mater.* 179 (2010) 251–257.
- [34] A.H. Sulaymon, W.M. Abood, Equilibrium and kinetic study of the adsorption of reactive blue, red, and yellow dyes onto activated carbon and barley husk, *Desalin. Water Treat.* 52 (2013) 1–9.
- [35] M. Shirmardi, A.H. Mahvi, A. Mesdaghinia, S. Nasser, R. Nabizadeh, Adsorption of acid red18 dye from aqueous solution using single-wall carbon nanotubes: Kinetic and equilibrium, *Desalin. Water Treat.* 51 (2013) 6507–6516.
- [36] M. Ghaedi, B. Sadeghian, A.A. Pebdani, R. Sahraei, A. Daneshfar, C. Duran, Kinetics, thermodynamics and equilibrium evaluation of direct yellow 12 removal by adsorption onto silver nanoparticles loaded activated carbon, *Chem. Eng. J.* 187 (2012) 133–141.
- [37] S.R. Chowdhury, E.K. Yanful, Arsenic removal from aqueous solutions by adsorption on magnetite nanoparticles, *Water Environ. J.* 25 (2011) 429–437.
- [38] S. Senthilkumaar, P. Kalaamani, K. Porkodi, P. Varadarajan, C. Subburaam, Adsorption of dissolved reactive red dye from aqueous phase onto activated carbon prepared from agricultural waste, *Bioresour. Technol.* 97 (2006) 1618–1625.
- [39] M.A. Ahmad, N.K. Rahman, Equilibrium, kinetics and thermodynamic of Remazol Brilliant Orange 3R dye adsorption on coffee husk-based activated carbon, *Chem. Eng. J.* 170 (2011) 154–161.
- [40] M. Yazdanbakhsh, I. Khosravi, E.K. Goharshadi, A. Youssefi, Fabrication of nanospinel ZnCr_2O_4 using sol-gel method and its application on removal of azo dye from aqueous solution, *J. Hazard. Mater.* 184 (2010) 684–689.
- [41] A. Roy, J. Bhattacharya, A binary and ternary adsorption study of wastewater Cd(II), Ni(II) and Co(II) by $\gamma\text{-Fe}_2\text{O}_3$ nanotubes, *Sep. Purif. Technol.* 115 (2013) 172–179.
- [42] Y. Kalpakli, Ş. Toygun, G. Köneçoğlu, M. Akgün, Equilibrium and kinetic study on the adsorption of basic dye (BY28) onto raw Ca-bentonite, *Desalin. Water Treat.* 52 (2013) 1–11.
- [43] E.L. Foletto, G.C. Collazzo, M.A. Mazuttia, S.L. Jahna, Adsorption of textile dye on zinc stannate oxide: Equilibrium, kinetic and thermodynamics studies, *Sep. Sci. Technol.* 46 (2011) 2510–2516.
- [44] M.A.P. Cechinel, S.M.A.G. Ulson de Souza, A.A. Ulson de Souza, Study of lead (II) adsorption onto activated carbon originating from cow bone, *J. Clean Prod.* 65 (2014) 342–349.